Supporting Information

A DFT Study on the Catalytic CO Oxidative Coupling to Dimethyl Oxalate on Al-Doped Core-Shell Pd Clusters

Xue Feng[†], Lixia Ling[*,†,‡], Yueting Cao[†], Riguang Zhang[§], Maohong Fan[‡], Baojun Wang[*, §]

[†] College of Chemistry and Chemical Engineering, Taiyuan University of Technology, Taiyuan 030024, Shanxi, People's Republic of China

[‡] Department of Chemical and Petroleum Engineering, University of Wyoming, 1000 E University Ave, Laramie, WY 82071, USA

[§] Key Laboratory of Coal Science and Technology (Taiyuan University of Technology), Ministry of Education and Shanxi Province, Taiyuan 030024, Shanxi, People's Republic of China

Adsorption configurations of possible species involving in CO oxidative coupling to DMO together with the corresponding adsorption energies ($kJ \cdot mol^{-1}$) on Pd_{13}, $Al@Pd_{12}$ and $Ag@Pd_{12}$ are shown in **Figure S1~ S3**.

Potential energy diagrams in all elementary reaction of CO oxidative coupling to DMO, and structures of initial states, transition states and final states on Pd_{13} catalyst are shown in **Figure S4~ S8**.

Potential energy diagrams of the reaction of CO oxidative coupling to DMO, as well as structures of initial states, transition states and final states on Pd_{13}, $Al@Pd_{12}$ and $Ag@Pd_{12}$ are shown in **Figure S9~ S11**.

Adsorption configurations of possible species involving in CO oxidative coupling to DMO together with the corresponding adsorption energies ($kJ \cdot mol^{-1}$) on $Al_6@Pd_{32}$ and $Al_{13}@Pd_{42}$ are shown in **Figure S12~ S13**.

[*] Corresponding author at: No. 79 West Yingze Street, Taiyuan 030024, China. Tel.: +86 351 6010898; Fax: +86 351 6041237

E-mail address: linglixia@tyut.edu.cn (L.X. Ling); wangbaojun@tyut.edu.cn (B.J. Wang)

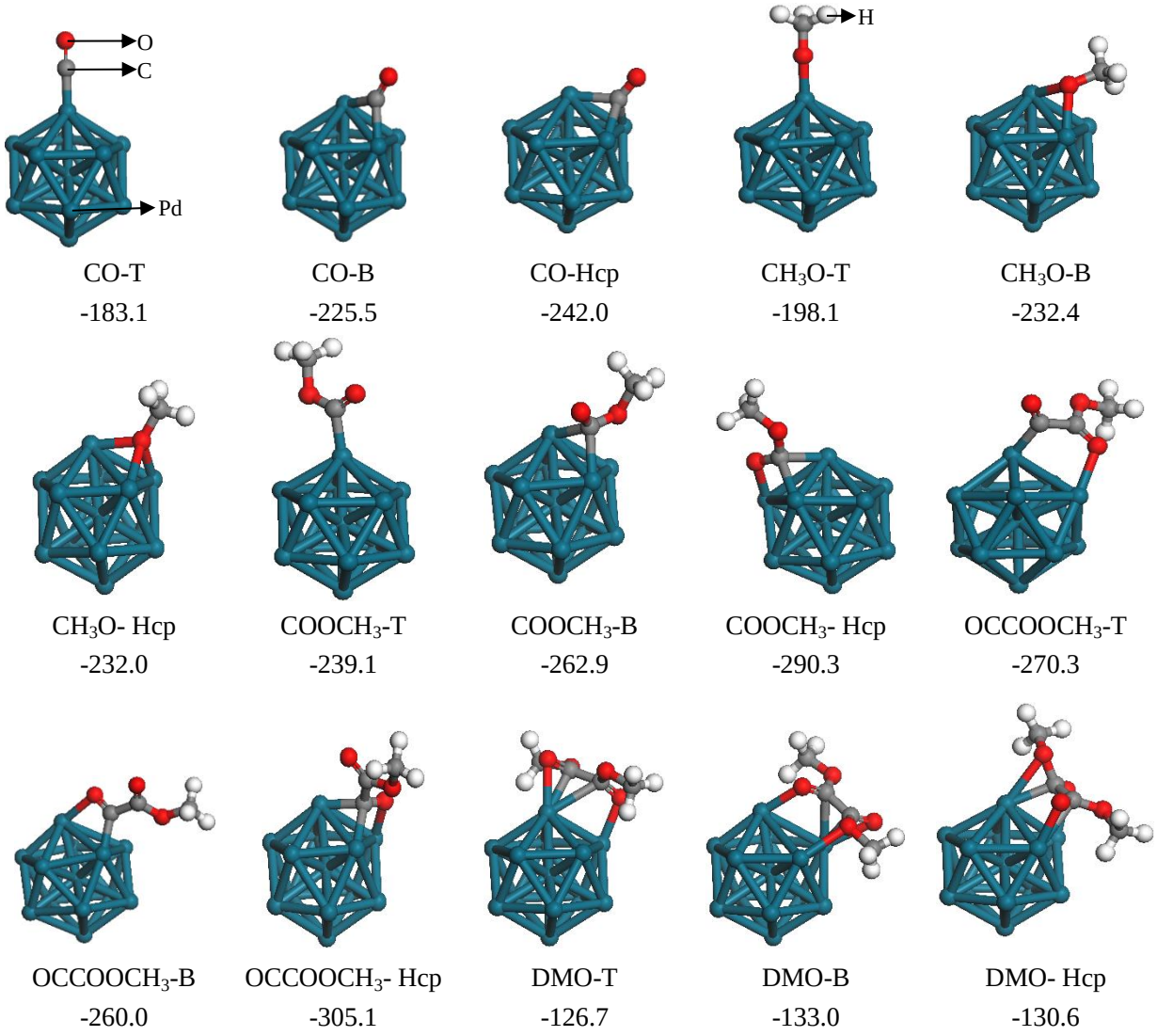

Figure S1. Adsorption configurations of possible species involving in CO oxidative coupling to DMO on Pd_{13} cluster together with the corresponding adsorption energies ($kJ \cdot mol^{-1}$).

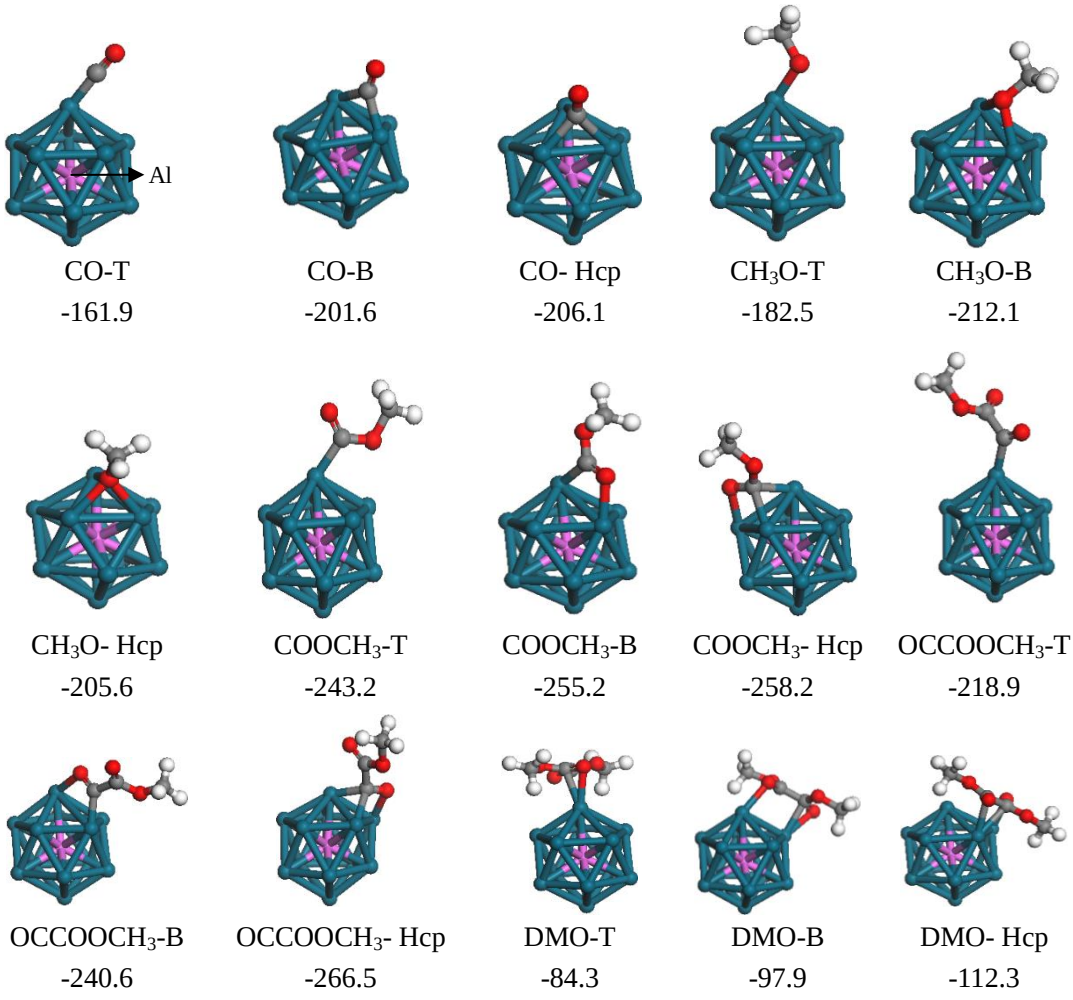

Figure S2. Adsorption configurations of possible species involving in CO oxidative coupling to DMO on $Al@Pd_{12}$ core-shell bimetallic cluster together with the corresponding adsorption energies ($kJ \cdot mol^{-1}$).

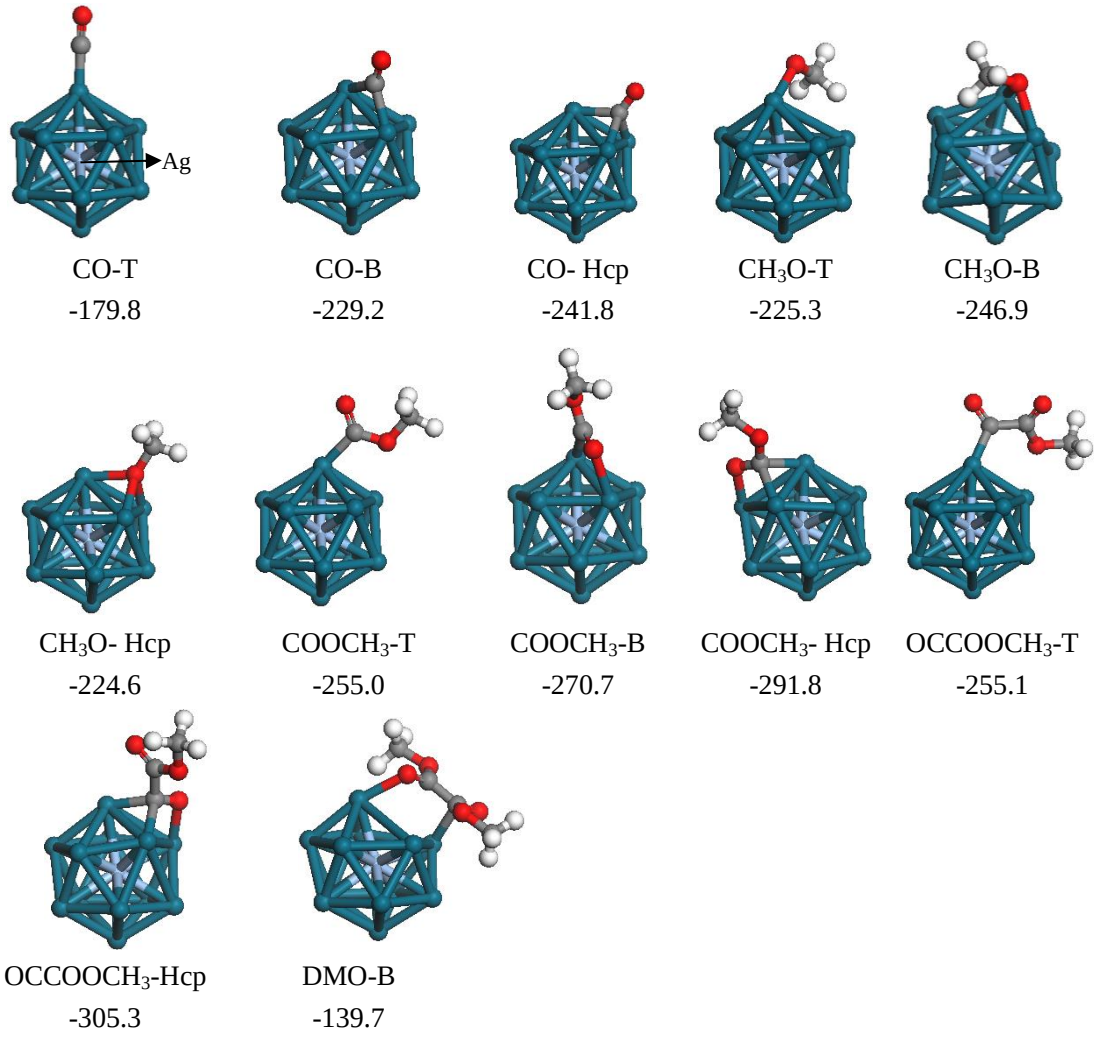

Figure S3. Adsorption configurations of possible species involving in CO oxidative coupling to DMO on $Ag@Pd_{12}$ core-shell bimetallic cluster together with the corresponding adsorption energies ($kJ \cdot mol^{-1}$).

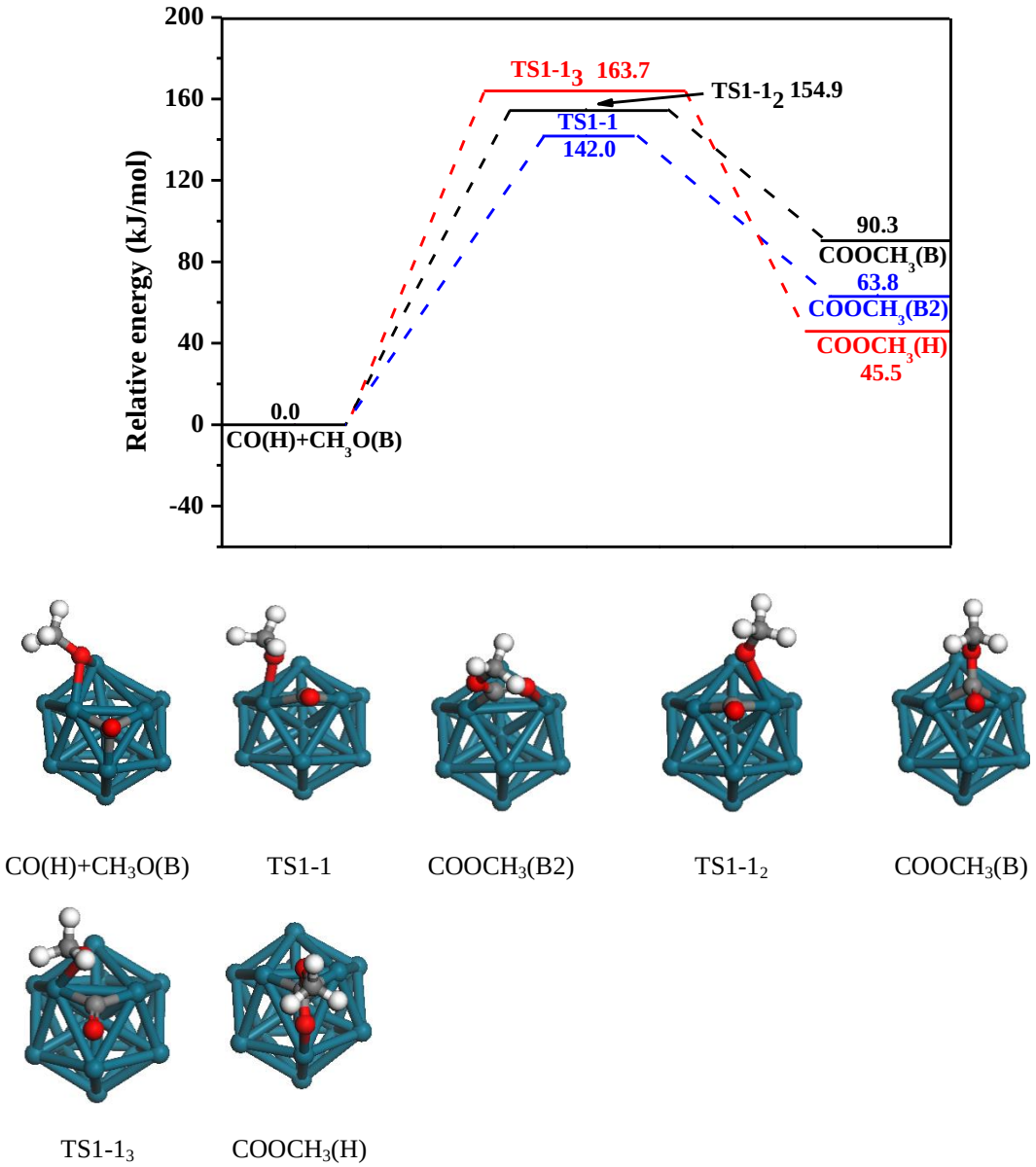

Figure S4. Potential energy diagram in the reaction of CO + CH_3O →$COOCH_3$, and structures of initial states, transition states and final states on Pd_{13} catalyst.

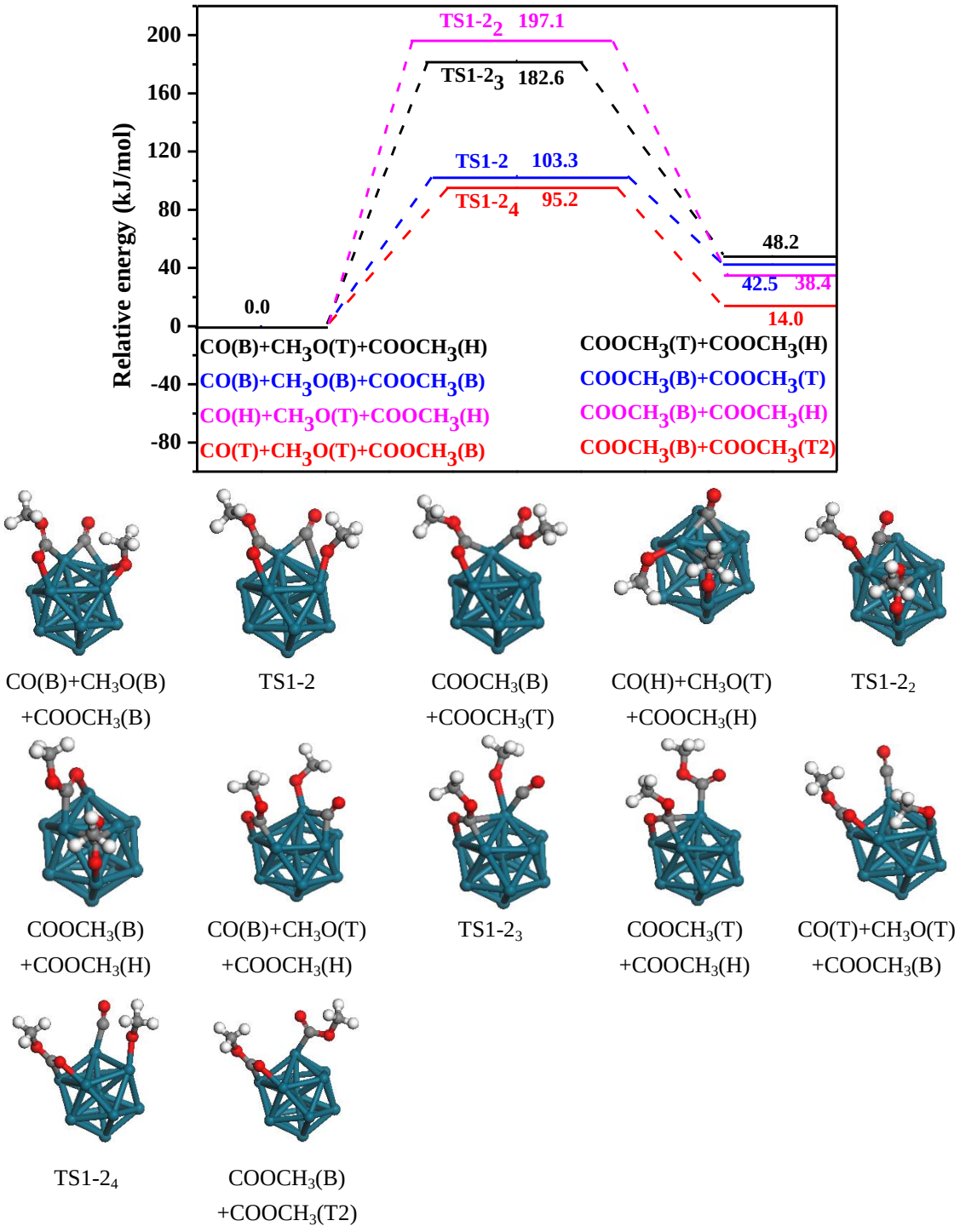

Figure S5. Potential energy diagram in the reaction of CO + CH_3O + $COOCH_3$ →$COOCH_3$ + $COOCH_3$, and structures of initial states, transition states and final states on Pd_{13} catalyst.

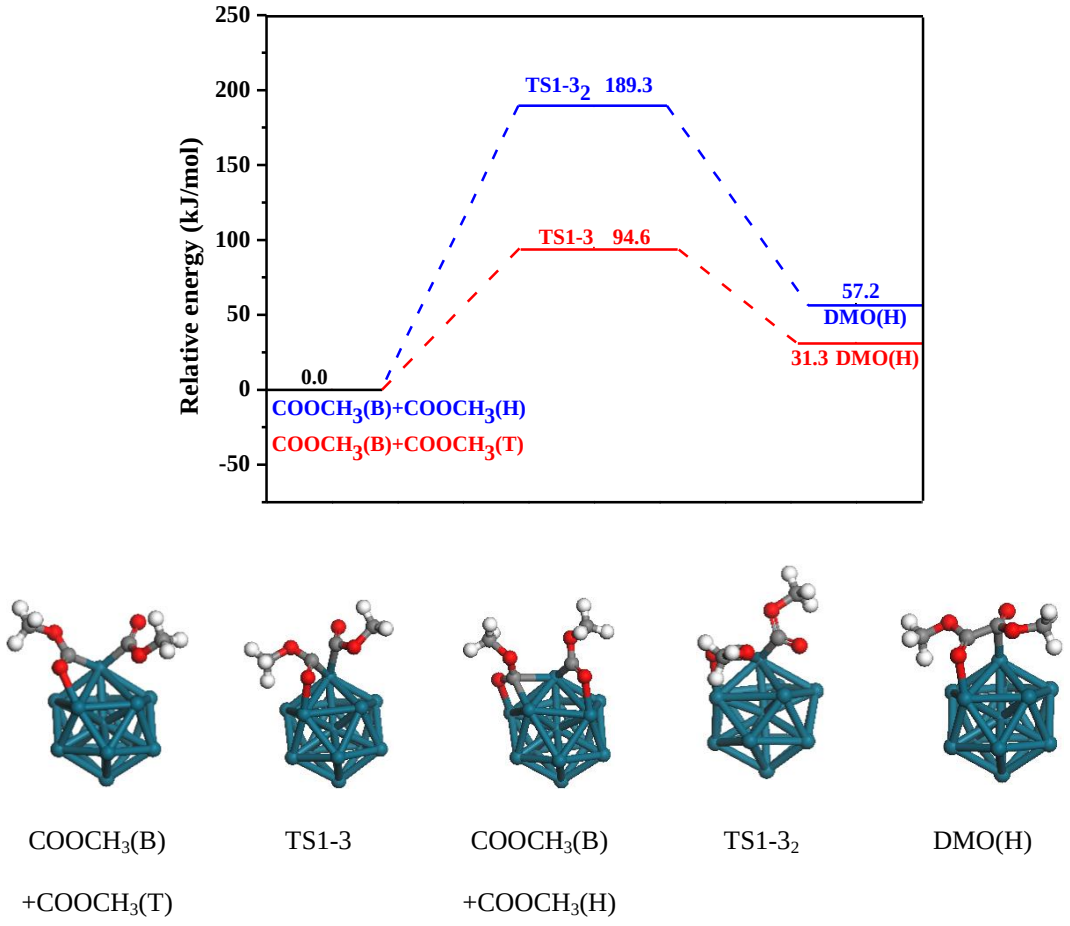

Figure S6. Potential energy diagram in the reaction of $COOCH_3$+$COOCH_3$ → DMO, and structures of initial states, transition states and final states on Pd_{13} catalyst.

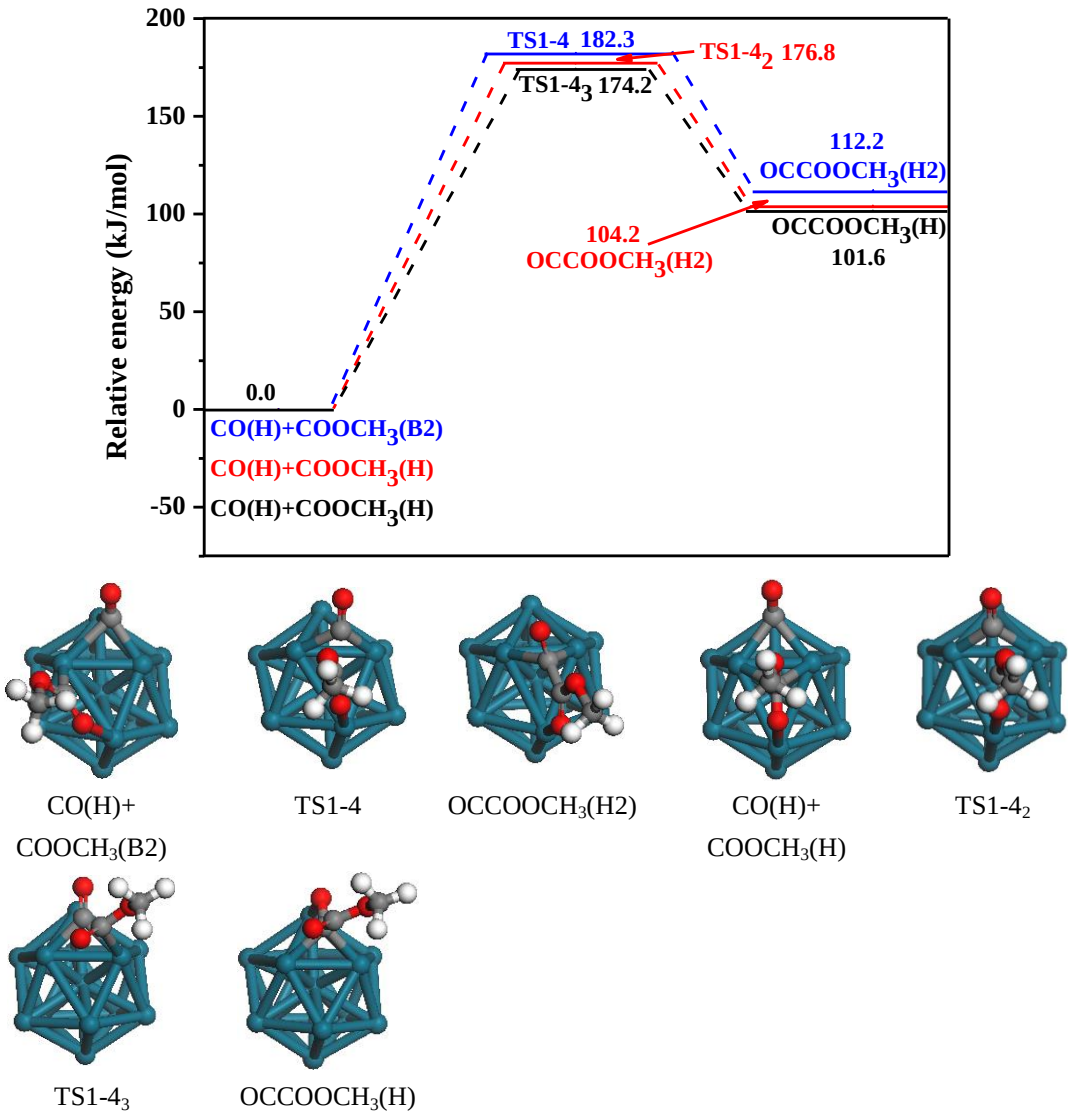

Figure S7. Potential energy diagram in the reaction of $CO+COOCH_3 \rightarrow OCCOOCH_3$, and structures of initial states, transition states and final states on Pd_{13} catalyst.

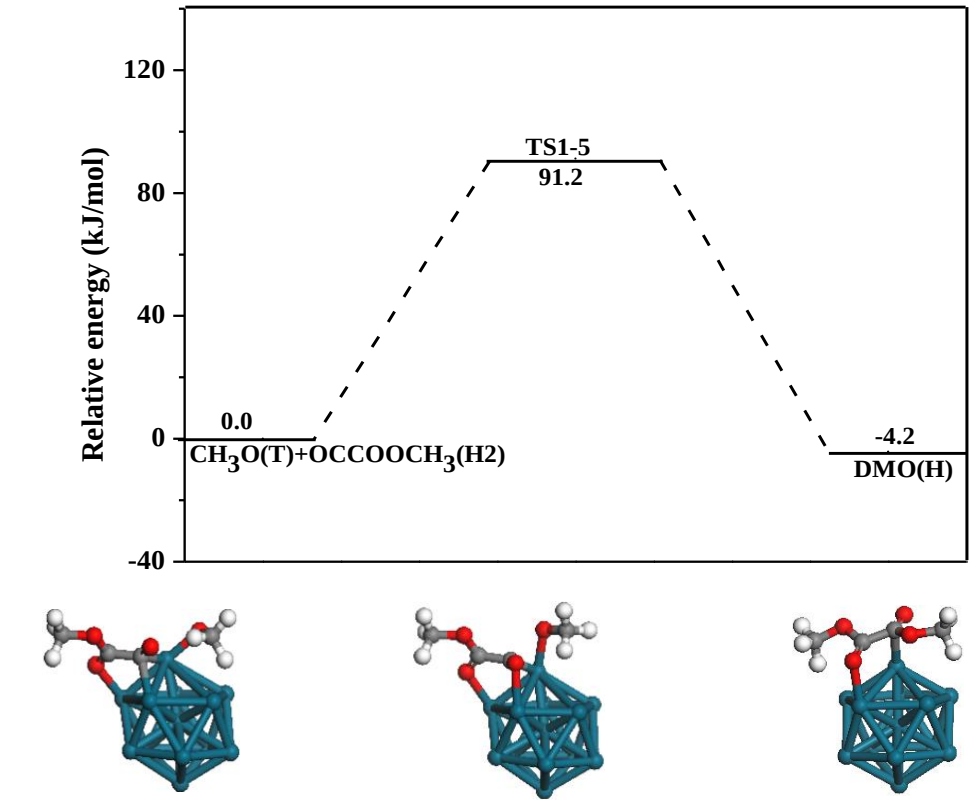

Figure S8. Potential energy diagram in the reaction of CH_3O + $OCCOOCH_3$ →DMO, and structures of initial states, transition states and final states on Pd_{13} catalyst.

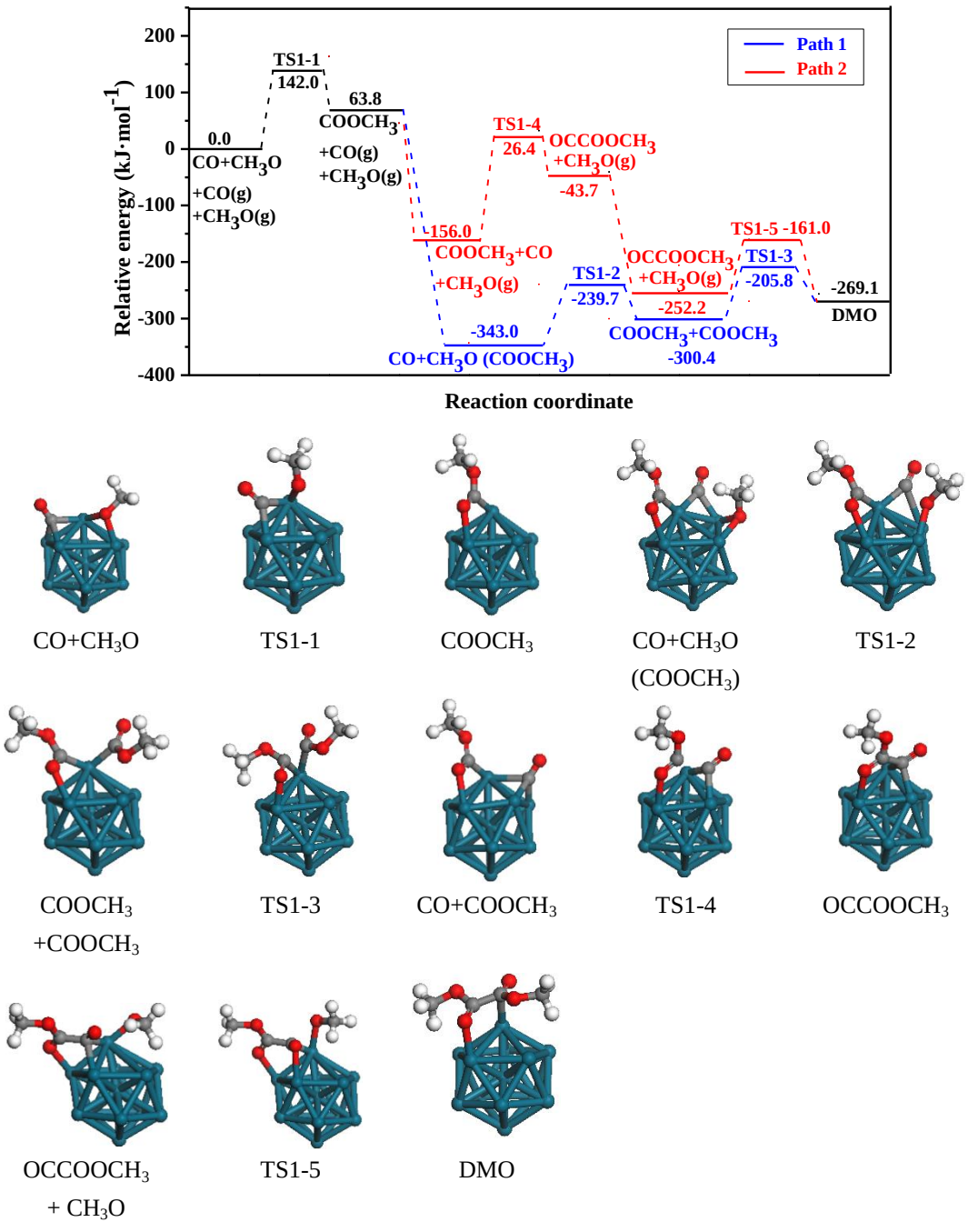

Figure S9. Potential energy diagram in the reaction of CO oxidative coupling to DMO, and structures of initial states, transition states and final states on Pd_{13} catalyst.

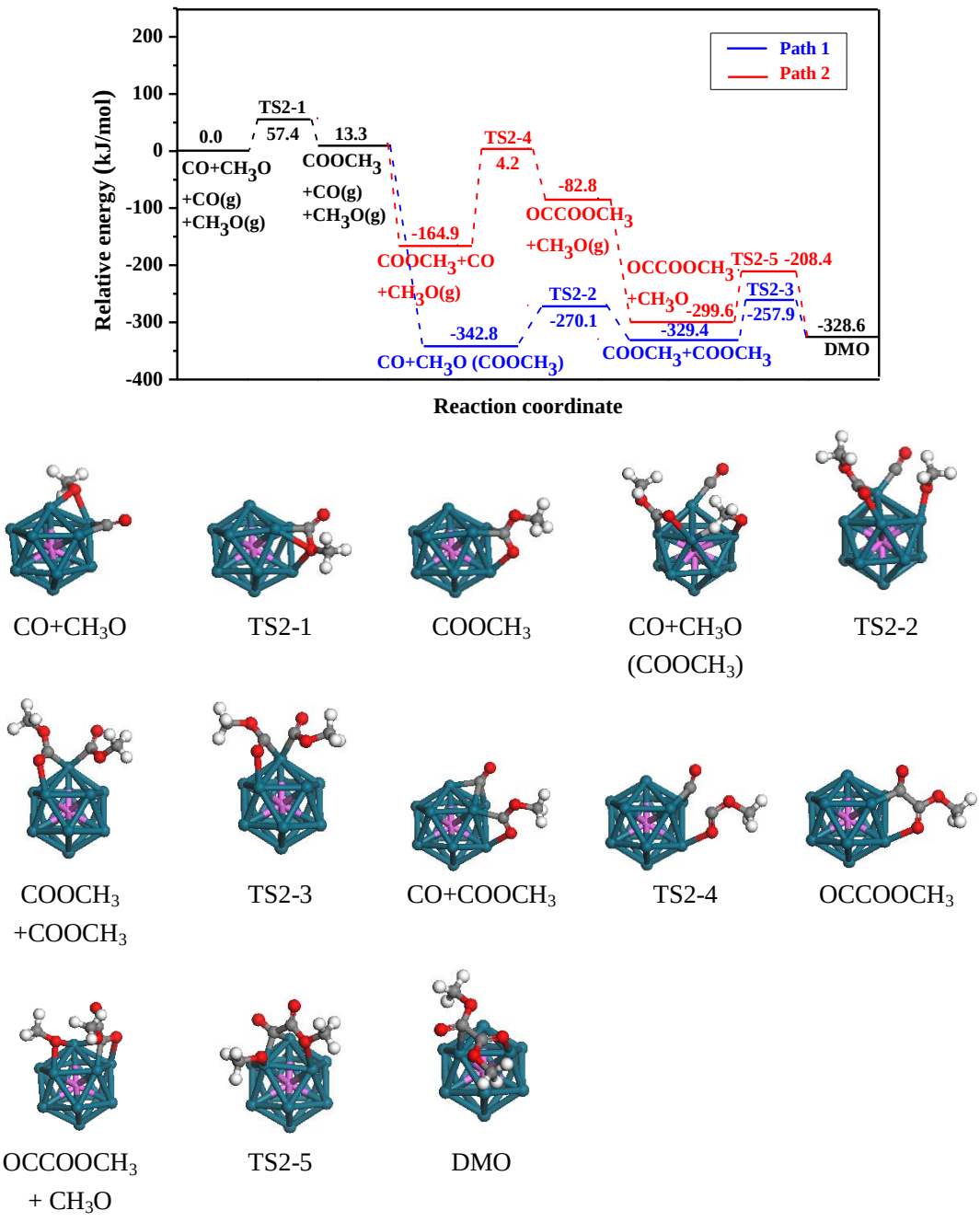

Figure S10. Potential energy diagram in the reaction of CO oxidative coupling to DMO, and structures of initial states, transition states and final states on $Al@Pd_{12}$ core-shell bimetallic catalyst.

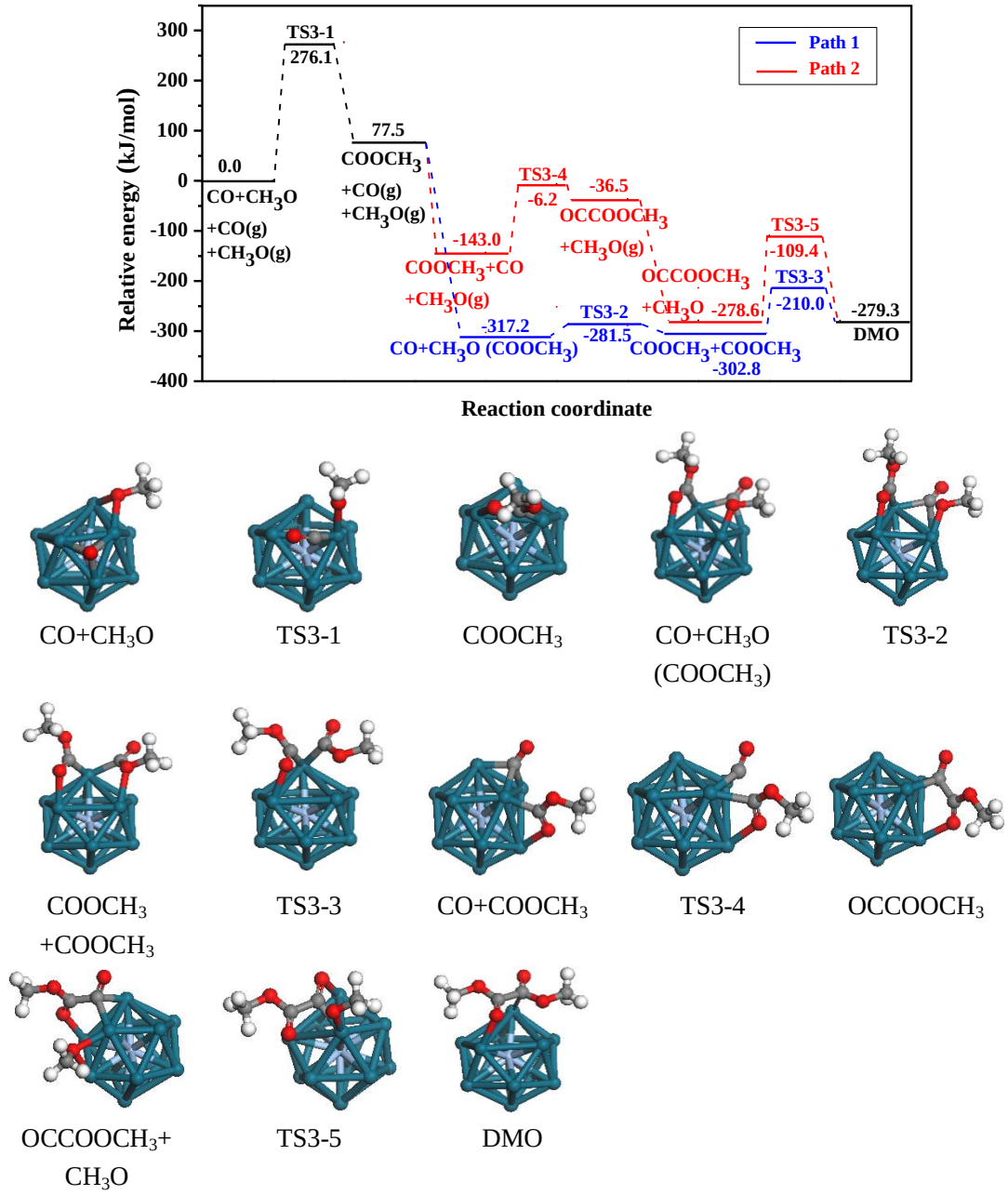

Figure S11. Potential energy diagram in the reaction of CO oxidative coupling to DMO, and structures of initial states, transition states and final states on $Ag@Pd_{12}$ core-shell bimetallic catalyst.

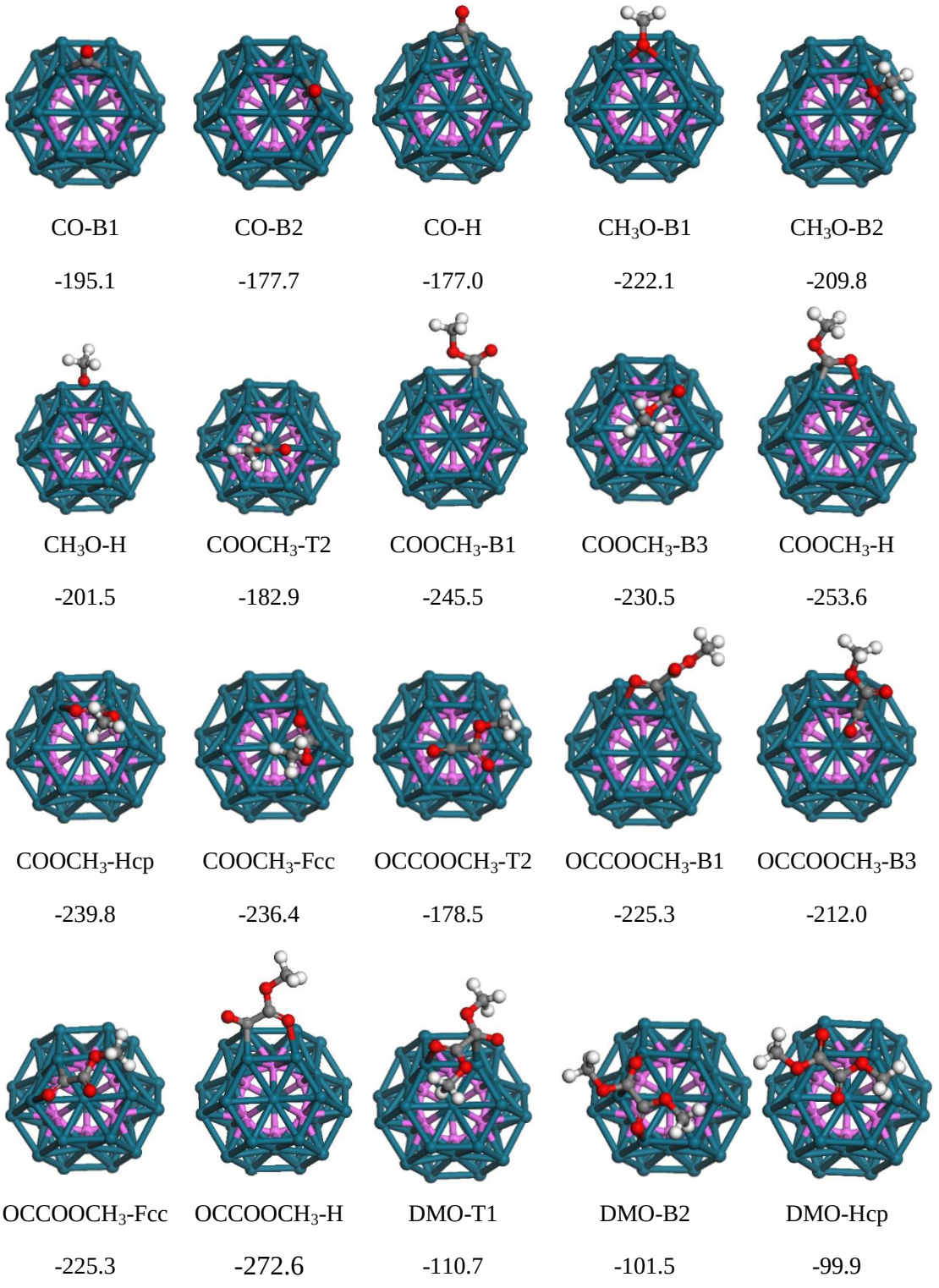

Figure S12. Adsorption configurations of possible species involving in CO oxidative coupling to DMO on $Al_6@Pd_{13}$ core-shell bimetallic cluster together with the corresponding adsorption energies ($kJ \cdot mol^{-1}$).

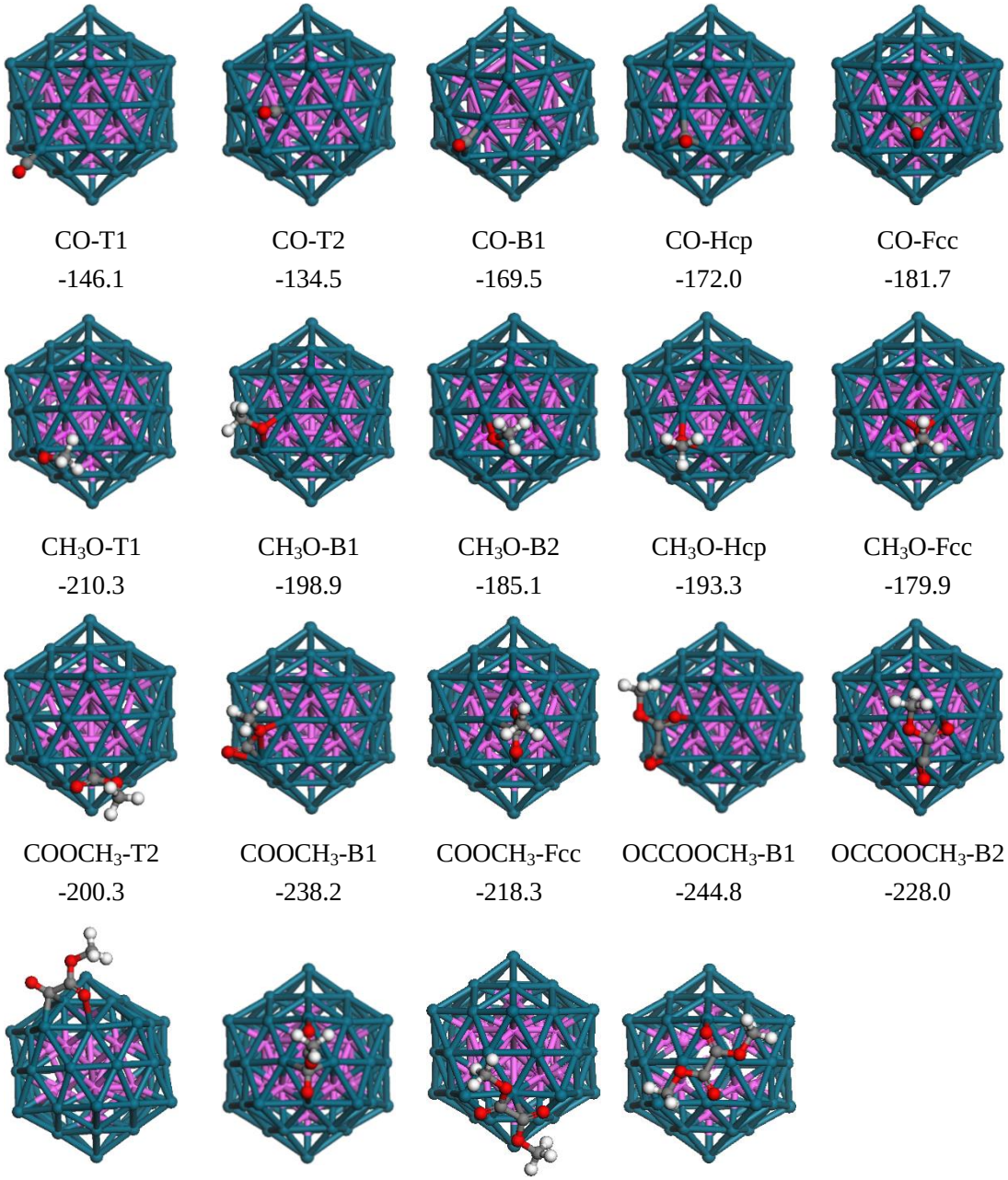

Figure S13. Adsorption configurations of possible species involving in CO oxidative coupling to DMO on $Al_{13}@Pd_{42}$ core-shell bimetallic clusters together with the corresponding adsorption energies ($kJ \cdot mol^{-1}$).